RSC Advances

PAPER

View Article Online
View Journal | View Issue

Cite this: *RSC Adv.*, 2020, **10**, 40365

Improved conversion of bamboo shoot shells to furfuryl alcohol and furfurylamine by a sequential catalysis with sulfonated graphite and biocatalysts†

Xiao-Qing Feng,‡[a] Yuan-Yuan Li,‡[a] Cui-Luan Ma,‡[ab] Yan Xia[a] and Yu-Cai He *[abc]

Received 28th August 2020
Accepted 22nd October 2020

DOI: 10.1039/d0ra07372e

rsc.li/rsc-advances

Furfurylamine and furfuryl alcohol are known as important furfural-upgrading derivatives in the production of pharmaceuticals, fibers, additives, polymers, *etc.* In a one-pot manner, the catalysis of biomass into furan-based chemicals was established in a tandem reaction with sulfonated Sn–graphite catalysts and biocatalysts. Using a raw bamboo shoot shell (75.0 g L^{-1}) as the feedstock, a high furfural yield of 41.1% (based on xylan) was obtained using the heterogeneous Sn–graphite catalyst (3.6 wt% dosage) in water (pH 1.0) for 30 min at 180 °C. Under the optimum bioreaction conditions, the biomass-derived furfural could be transformed into furfuryl alcohol (0.310 g furfuryl alcohol per g xylan in biomass) by a reductase biocatalyst or furfurylamine (0.305 g furfurylamine per g xylan in biomass) using an ω-transaminase biocatalyst. Such one-pot chemoenzymatic processes combined the merits of both heterogeneous catalysts and biocatalysts, and sustainable processes were successfully constructed for synthesizing key bio-based furans.

1. Introduction

The global trend is aimed at developing numerous environmentally friendly technologies for utilizing sustainable and abundant lignocellulosic biomass to manufacture numerous functional materials, biofuels, and chemicals as substitutes to the current petroleum-based economy.[1–4] A bamboo shoot shell (BSS) is mainly composed of carbohydrate (hemicellulose plus cellulose) and lignin. It is an abundant renewable bioresource of energy, food, feed and chemicals, which has an annual output of about 20 million tons in China.[5] However, most of BSSs are burned or directly discarded and are not yet effectively utilized, which cause waste of resources and environmental pollution.

Furfural (FF) is known as one of the top twelve value-added platform bio-chemicals that can be synthesized from renewable biomass.[3] It has been widely utilized in the industrial production of additives, solvents, biofuels, plastics, resins, and polymers.[6–9] FF is also used as a building block for the synthesis of high-value-added furan-based chemicals such as furfuryl alcohol (FFA) and furfurylamine (FAM). FFA is an important FF derivative,[10,11] which can be utilized in manufacturing adhesives, vitamin C, plastics, dispersing agents, lubricants, polymers, resins and biofuels. Cu/MgO gave 98% yield of FFA at 180 °C under high-pressured H_2.[12] A nickel–tin-based catalyst converted FF to FFA (99% selectivity) at 100 °C in the presence of high-pressured H_2 (2.0 MPa) in a biphasic system.[13] UiO-66 converted FF to FFA (71% yield) for 10 h at 170 °C.[14] Another FF-upgrading product FAM is a useful compound in the production of drugs, additives, fibers and pesticides, which can be prepared by the amination of FF and the reduction of CN- or NO_3-based compounds over chemical catalysts.[15–17] Ru/HZSM-5 catalyzed FF into FAM at 76% yield at 100 °C under high-pressurized H_2 (3.0 MPa).[18]

Recently, it has gained an increase in interest to synthesize furan-based chemicals *via* biocatalysis approaches. To efficiently catalyze BSS into furans (FFA and FAM), a tandem catalysis of BSS was established *via* the chemoenzymatic approach using a heterogeneous catalyst and biocatalyst (reductase or ω-transaminase) (Fig. 1). Heterogeneous Sn–graphite was first prepared and further characterized *via* SEM, XRD, FTIR and BET, and then, the effects of catalytic system's pH, catalytic temperature, catalytic time and catalyst Sn–graphite dosage on the FF production were investigated. Moreover, biotransformation conditions for converting FF to high-value-added furan (FFA or FAM) by recombinant reductase or ω-transaminase were optimized. Finally, one-pot catalytic processes for catalyzing BSS into furan-based chemicals (FAM and FOL) were established in the tandem catalytic reaction with sulfonated Sn–graphite catalysts and biocatalysts.

[a]*Biomass and Bioenergy Laboratory, School of Pharmacy, Changzhou University, Changzhou, P. R. China. E-mail: heyucai2001@163.com*

[b]*State Key Laboratory of Biocatalysis and Enzyme Engineering, School of Life Sciences, Hubei University, Wuhan, P. R. China*

[c]*Jiangsu Key Laboratory for Biomass-Based Energy and Enzyme Technology, Huaiyin Normal University, Huaian, P. R. China*

† Electronic supplementary information (ESI) available. See DOI: 10.1039/d0ra07372e

‡ Xiao-Qing Feng, Yuan-Yuan Li and Cui-Luan Ma have contributed equally to this manuscript.

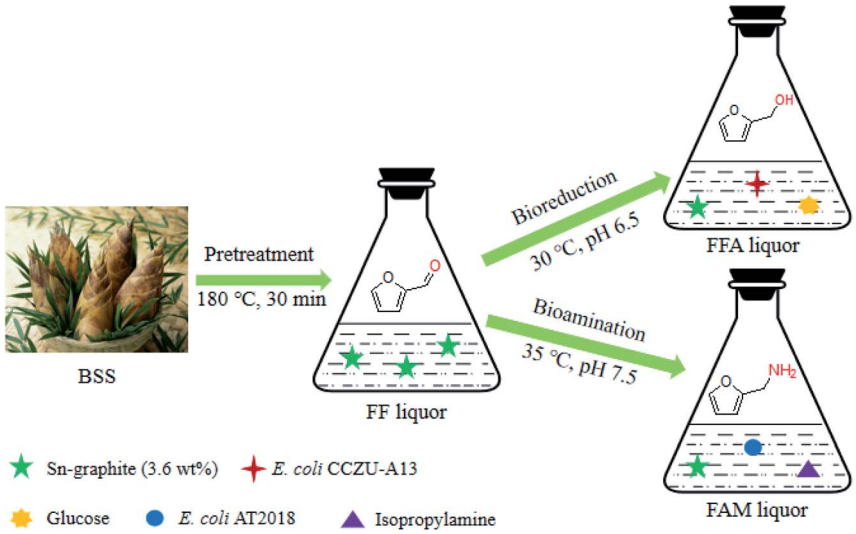

Fig. 1 Tandem catalysis of BSS to FFA or FAM *via* a chemoenzymatic approach.

2. Materials and methods

2.1. Materials

A bamboo shoot shell (BSS) was collected from a village (Changzhou, China). Graphite was purchased from Jinglong Graphite Factory (Beijing, China). $SnCl_4 \cdot 5H_2O$, ammonia, isopropylamine (IPA), furfural (FF) and other chemicals were purchased from Changzhou Runyou Reagent Co., Ltd. (Jiangsu, China) and other commercial sources.

2.2. Synthesis of the Sn–graphite catalyst

50.0 g of raw graphite was immersed in 150 mL of 4.0 M H_2SO_4 at 60 °C for 3.5 h. Subsequently, the pH of this mixture was regulated to neutrality, and the acid-treated graphite was isolated by filtration and washed by deionized water to remove residues. 19.4 g of $SnCl_4 \cdot 5H_2O$, 42.0 g of acid-treated graphite, and 700 g of ethanol were added to a 2 L container and thoroughly blended by stirring. Aqueous ammonia $NH_3 \cdot H_2O$ (25.0 wt%) was slowly dropped into the emulsion, and its pH was regulated to reach 6.0. This pH-adjusted solution was dried in a 70 °C oven for 12 h and further oven-dried for another 12 h at 90 °C. 150 mL of 0.50 M H_2SO_4 immersed dried solid powder for 3 h, and then, this sulfonated solid was isolated by filtration and washed by deionized water to neutrality. Wet solid was dried in a 110 °C oven for 3 h and further dried in a 500 °C muffle furnace for another 3 h. Sn–graphite was obtained for further use.

2.3. Sn–graphite-mediated catalysis of BSS to FF

Dry-milled BSS (3.75 g, 40–60 mesh), Sn–graphite (0–6.0 wt% dosage) and 50 mL water were blended in a 100 mL high-temperature and high-pressure (HTHP) stainless-steel reactor (Zhengjiang Jingkou Dantu Huanqiu Electrical Instrument, P. R. China). After BSS were catalyzed for 5–60 min at a certain temperature (160–180 °C) and pH (0.6–1.2) under 500 rpm agitation, this reactor was placed in an iced water-bath. The formed FF was measured by HPLC. FF yield from xylan in BSS was calculated using the following equation:

$$\text{FF yield } (\%) = \frac{\text{FF produced (g)} \times 0.88}{\text{BSS (g)} \times 0.283} \times \frac{150}{96} \times 100$$

2.4. Biosynthesis of FFA and FAM from FF

The bioreduction of FF was conducted by recombinant *E. coli* CCZU-A13 expressing an NADH-dependent reductase.[19] The bioamination of FF was carried out by recombinant *E. coli* AT2018 cells harboring ω-transaminase.[2] In a 100 mL Luria–Bertani (LB) broth containing 50.0 μg mL^{-1} kanamycin, the cells were grown to optical density at 600 nm (OD_{600}) of 0.60 at 37 °C and induced with the addition of IPTG (50.0 μmol). After incubation at 37 °C for another 5 h, the cells were harvested in a centrifuge at 4 °C and 9000 × *g* for 6 min, and then washed with 0.85 wt% normal saline three times.

In this study, the catalytic conversions of FF were pH and temperature that affecting FF biotransformation were optimized using commercial FF (60.0 mM) as the substrate. FF-reducing reactions were carried out in various pH values of buffers (100 mM, pH 6.5–8.0) with CCZU-A13 cells (50.0 g L^{-1}) in the presence of cosubstrate glucose (0.5–3.0 mol glucose per mol FF) at 20–45 °C. Bioamination reactions were conducted in various pH values of buffers (100 mM, pH 6.5–9.0) with AT2018 cells (50.0 g L^{-1}) in the presence of amine donor isopropylamine (IPA) (0.50–5.0 mol IPA per mol FF) at 25–50 °C. FF, FFA and FAM were assayed *via* HPLC.

Dry-milled BSS (3.75 g, 40–60 mesh), Sn–graphite (3.6 wt%) and 50 mL water were blended in a 100 mL HTHP reactor. After BSS were catalyzed in this media (pH 1.0) for 30 min at 180 °C and 500 rpm, the pH of the FF liquor was regulated to suitable pH for biotransformation. The bioreduction of FF into FFA with *E. coli* CCZU-A13 wet cells (50.0 g L^{-1}) was conducted at pH 6.5 and 30 °C in the presence of cosubstrate glucose (1 mol glucose per mol FF). The bioamination of FF into FAM with *E. coli*

Table 1 Surface and pore changes of Sn–graphite and graphite

Graphite sample	BET surface area, $m^2\ g^{-1}$	Pore volume, $cm^3\ g^{-1}$	Pore size, nm
Sn–graphite	30.4	0.04	5.1
Fresh graphite	0.6	0.02	138.0

AT2018 wet cells (50.0 g L^{-1}) was conducted at pH 7.5 and 35 °C in the presence of amine donor IPA (3 mol IPA per mol FF).

$$\text{FFA yield (\%)} = \frac{\text{FFA produced (mM)}}{\text{Initial FF (mM)}} \times 100$$

$$\text{FAM yield (\%)} = \frac{\text{FAM produced (mM)}}{\text{Initial FF (mM)}} \times 100$$

2.5. Analytical methods

Graphite or Sn–graphite was observed *via* Fourier transform infrared spectroscopy using Nicolet PROTÉGÉ FT-IR (JSM-6360LA, JEOL, Japan), X-ray diffraction (XRD) on a Rigaku XRD-6000 diffractometer (Rigaku Corporation, Japan) with a CuKα radiation and JCPDS reference number (no. 85-0712), and scanning electron microscopy (SEM) (JSM-6360LA, JEOL, Japan). In an ASAP2020M system (Micromeritics Instrument Co., USA), nitrogen adsorption–desorption isotherms at 77 K were used to measure the Brunauer–Emmett–Teller (BET)-specific surface area. The X-ray photoelectron spectroscopy (XPS) analysis was performed on a physical electronics ESCALAB 250 spectrometer (Thermo Fisher Scientific Co. Ltd, USA). FF, FFA, and FAM were quantified *via* HPLC.[20,21] FF (furfural), FAM (furfurylamine), and FFA (furfuryl alcohol) were determined by HPLC equipped with a Waters Nova-Pak C18 column (3.9 × 150 mm, 4 μM), which were eluted by mobile phase (20 v% methanol and 80 v% water containing 0.1 wt% trifluoroacetic acid) at a flow rate of 0.8 mL min^{-1}. FFA and FAM were detected at 210 nm, and FF was detected at 254 nm. The components of BSS were determined as reported NREL (National Renewable Energy Laboratory) method (http://www.nrel.gov/biomass/analytical_procedures.html).

3. Results and discussion

3.1. Characterization of solid acid Sn–graphite

Graphite, one highly promising carrier, has currently been used for the preparation of functional materials, adsorbents, catalysts, *etc.*[22–25] In this case, tin-loaded sulfonated acid-treated graphite (Sn–graphite) was used to convert BSS into FF. The surface changes of Sn–graphite were observed by nitrogen adsorption–desorption isotherms, XRD, SEM and FT-IR.

Nitrogen adsorption–desorption isotherms were used to examine the changes of the Sn–graphite surface area, and the results are given in Table 1. Sn–graphite had a smaller pore size (5.1 nm), larger BET specific surface area (30.4 $m^2\ g^{-1}$) and bigger pore volume (0.04 $cm^3\ g^{-1}$) compared to graphite. Probably, solvent treatment, sulfonation and oven-dry performance could change the pore and surface of graphite. SEM revealed that graphite and Sn–graphite had diverse distributions of particle size (Fig. 2). Chemical groups of graphite and Sn–graphite were observed *via* FT-IR (Fig. 3). The peaks at 3451 cm^{-1} (–OH stretching vibration),[26] 1632 cm^{-1} (the deformation mode of water molecules adsorbed on graphite surface),

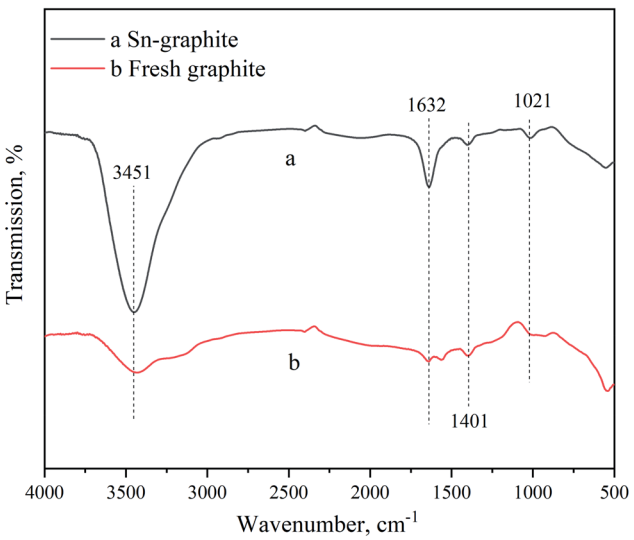

Fig. 3 FT-IR images of graphite and Sn–graphite.

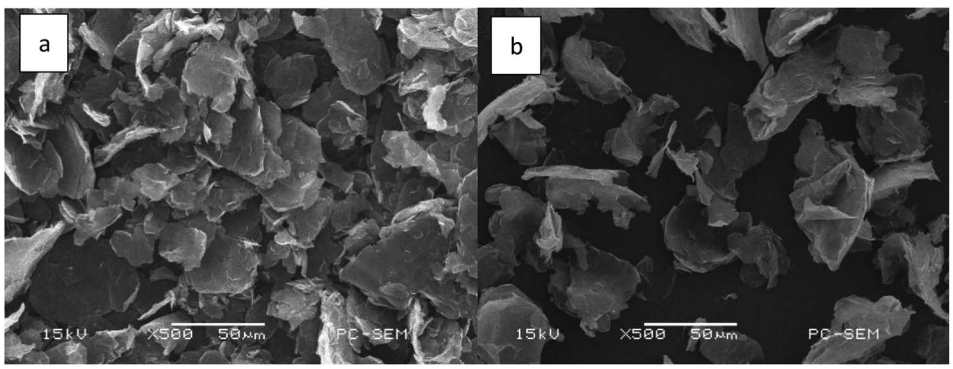

Fig. 2 SEM images of graphite (a) and Sn–graphite (b).

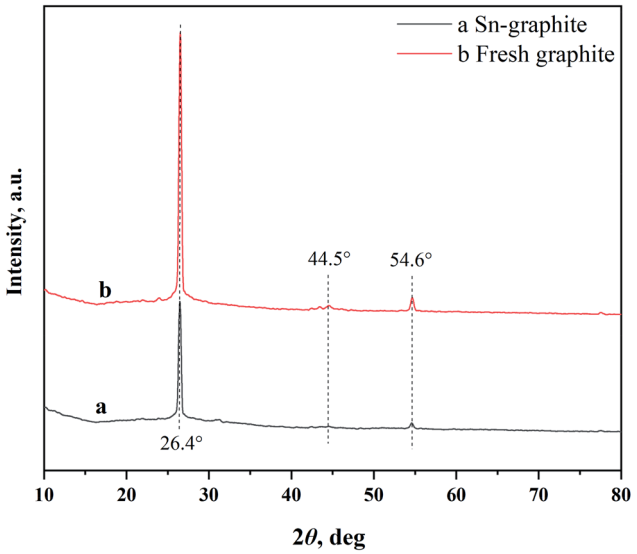

Fig. 4 XRD images of graphite and Sn–graphite.

1401 cm^{-1} (C–C stretching vibration), and 1021 cm^{-1} (stretching vibration of sulfur–oxygen double bonds of SO_4^{2-})[27] were observed. The FT-IR measurement was performed to understand the structure of Sn–graphite. This catalyst was sulfonated graphite. XRD was used to detect the crystal structures of solid samples (Fig. 4). Significant diffraction peaks at 2θ values of 26.4°, 44.5°, and 54.6° are observed in graphite and Sn–graphite. 2θ = 26.4° corresponds to the diffraction peak of graphite, which is also the characteristic peak of graphite. The peak intensities of Sn–graphite are lower than those of graphite. The Sn–graphite preparation process could influence the main structure of graphite. XPS was used for assaying Sn–graphite (Fig. S1, in ESI†). It was found that Sn had three valences (0, +2, and +4). The fractions of Sn^0 $3d_{5/2}$, Sn^0 $3d_{5/2}$, and Sn^0 $3d_{5/2}$ were 5.2%, 32.3%, and 63.5%, respectively. Graphite and tin exhibit very good biocompatibility and do not arise any serious toxicity. Using graphite, a heterogeneous tin-based graphite catalyst has the advantage over homogeneous catalysts due the potential biocompatible, easy to separate and high thermo-stability.

3.2. Optimization of catalyzing BSS into FF with Sn–graphite

Lignocellulosic biomass is a sustainable feedstock for manufacturing FF,[28,29] which involves the hydrolysis of xylan in biomass to D-xylose, followed by the dehydration of biomass-derived D-xylose to FF.[9] On an industrial scale, homogeneous mineral acids are widely used for converting D-xylose to FF; however, it encounters equipment corrosion, waste disposal and high operational cost.[30–32] To address these issues, numerous heterogeneous solid acids (Amberlyst 70, SBA-15-HSO_3, sulfonated attapulgite, functional resin, modified zeolite, *etc.*) exhibit superior catalytic characteristics for converting D-xylose into FF under environmentally friendly conditions.[33–38] To effectively catalyze biomass into FF, it was necessary to obtain the optimal solid acid-mediated conversion conditions. In this study, four catalytic reaction parameters including the catalytic system's acidity, catalytic temperature, catalytic time and catalyst Sn–graphite dosage were investigated for FF production.

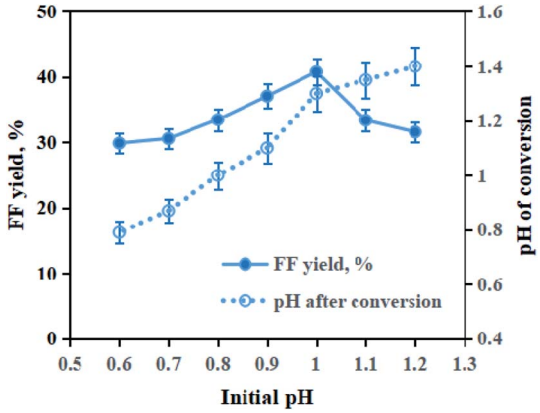

Fig. 5 Effects of the catalytic reaction system's pH on FF yields.

It is known that the degree of acidity in the catalytic reaction system may facilitate the FF formation.[1] Effects of the catalytic

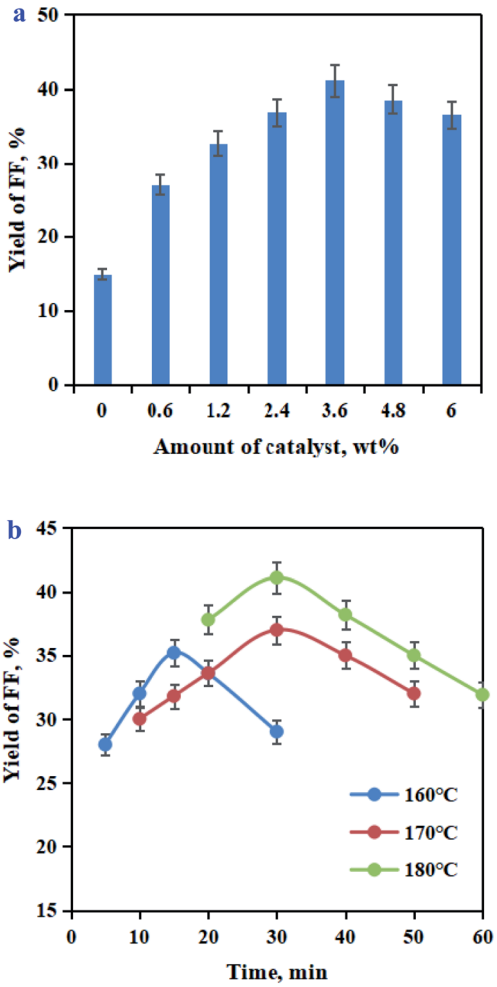

Fig. 6 Effects of the Sn–graphite catalyst's amount (a), catalytic time and catalytic temperature (b) on the FF yield.

system's pH (acidity) were tested on the FF yields within 30 min at 180 °C (Fig. 5). When the pH values were raised from 0.6 to 1.0, FF yields (based on xylan in BSS) increased from 29.9% to 41.1%. By raising the pH value from 1.0 to 1.2, FF yields decreased clearly. Too low pH of the catalytic system might result in FF degradation. After BSS samples were catalyzed with Sn–graphite in the HTHP reactor, the pH values of reaction media increased. Probably, the hydrolysis of xylan in BSS to pentose (mainly D-xylose) was required to consume H^+, and the dehydration of the formed D-xylose to FF produced H_2O. Therefore, the pH of the catalytic system was chosen as 1.0 for assisting the Sn–graphite-mediated conversion of BSS into FF.

In a catalytic reaction system, catalyst loading, catalytic temperature and catalytic time can influence the FF formation.[39–41] The catalytic process of BSS into FF was established in water (pH 1.0) containing Sn–graphite (0–6.0 wt% dose) at 160–180 °C for 5–60 min. It was found that Sn–graphite dosages had significance on the FF production (Fig. 6a). The yield of FF increased with the rise in the Sn–graphite dosage from 0 to 3.6 wt%, and the maximum (41.1% yield) at the dosage of 3.6 wt%. Further increasing the Sn–graphite dosage from 3.6 to 6.0 wt%, the FF yield dropped slowly. The effects of the catalytic temperature and time on the FF yields are illustrated in Fig. 6b. A high FF yield was achieved when BSS was converted for 30 min at 180 °C. Therefore, dry-milled BSS (75.0 g L^{-1}) was catalyzed with Sn–graphite (3.6 wt% dosage) in 50 mL water (pH 1.0) within 30 min at 180 °C. The obtained FF liquor was composed of 58.3 mM glucose, 50.0 mM xylose, 66.0 mM FF, 1.8 mM HMF, and 10.3 mM levulinic acid.

The results of the recycling test are shown in Fig. S2 (in ESI).† The FF yields decreased gradually after each recycle for 30 min at 180 °C. From 1st to 5th run, the yield of FF decreased from 41.1% to 36.1% in the sealed reactor, indicating a comparable stable recycle capacity. Sn–graphite had good stability to be reused for catalyzing BSS into FF. To further evaluate the stability of Sn–graphite, the determination of the Sn content was carried out before and after the repeated use of Sn–graphite (Table S1, in ESI†). The Sn content on Sn–graphite decreased slightly from 8.1% to 7.7% after the 1st recycle. However, the content of Sn ions on Sn–graphite dropped significantly to 2.9% after the 5th recycle. The loss of Sn on Sn–graphite resulted in a decrease in the FF yield after the recovery and reuse of Sn–graphite.

3.3. Biotransformation of FF into FFA and FAM

To efficiently synthesize FFA or FAM, the optimization of biologically transforming FF was conducted using 60.0 mM commercial FF as the substrate. Using CCZU-A13 cells as reductase biocatalysts, the optimum cosubstrate glucose, catalytic temperature and catalytic pH for catalyzing the bioreduction of FF were 1.0 mol glucose per mol FF, 30 °C and 6.5, respectively (Fig. S3 and S4, in ESI†). Using AT2018 cells as amination biocatalysts, the optimum amine donor IPA dose, the biocatalytic temperature and biocatalytic pH for the bioamination of FF were 3.0 mol IPA per mol FF, 35 °C and 7.5, respectively (Fig. S5 and S6, in ESI†).

In the HTHP reactor (500 rpm), dry-milled BSS (3.75 g), Sn–graphite (3.6 wt% dosage) and 50 mL water were blended and incubated for 30 min at 180 °C and pH 1.0. Subsequently, the pH of BSS-slurry containing 66.0 mM FF was regulated with 3 M NaOH. The bioreduction of BSS-derived FF was initiated by adding CCZU-A13 wet cells (50.0 g L^{-1}), which was conducted at pH 6.5 and 30 °C by the supplementary of glucose (1.0 mol glucose per mol FF). Without the removal of Sn–graphite, BSS-derived FF was completely catalyzed into FFA by CCZU-A13 whole cells within 2 h (Fig. 7a). *M. guilliermondii* catalyzed the bioreduction of 50.0 mM FF to FFA in the yield of 83%.[42] *B. coagulans* converted ~200.0 mM FF to FFA at 86% yield in a dioctyl phthalate–water biphasic system.[21] Significantly, CCZU-A13 whole-cells harbor high reductase activity towards FF in aqueous media. ω-Transaminase can synthesize organic amines *via* biotransamination. Aldehyde or ketone (amine acceptor) can accept the amino group ($-NH_2$) from an amine donor in the presence of coenzyme pyridoxal-5′-phosphate (PLP).[42–45] The bioamination of FF by AT2018 wet cells (50.0 g L^{-1}) was performed at pH 7.5 and 35 °C by the supplementary of amine donor IPA (3.0 mol IPA per mol FF). In the presence of Sn–graphite, BSS-derived FF was wholly catalyzed into FAM by AT2018 whole cells within 1.5 h (Fig. 7b). The yield of FAM reached 83% from 20.0 mM FF with *C. violaceum* within 24 h.[43]

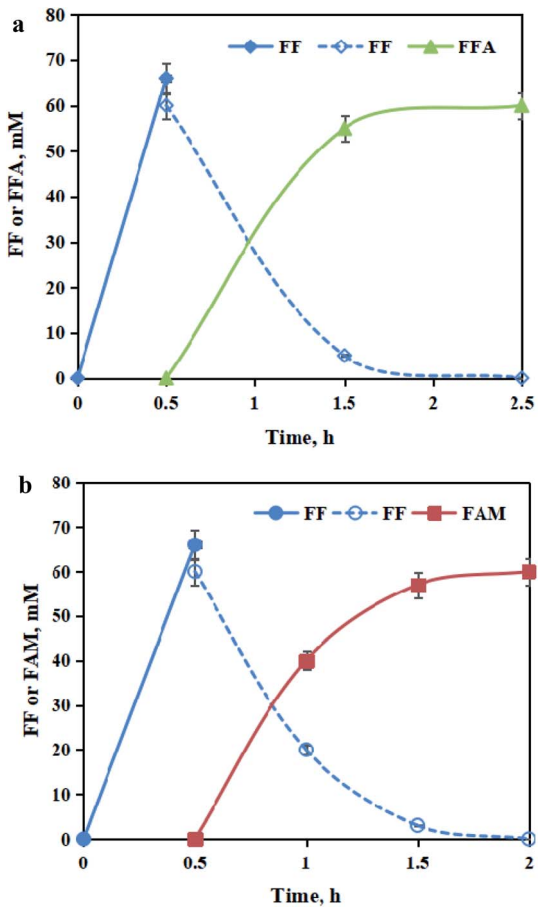

Fig. 7 Time courses for tandemly converting BSS into FFA (a); time courses for tandemly converting BSS into FAM (b).

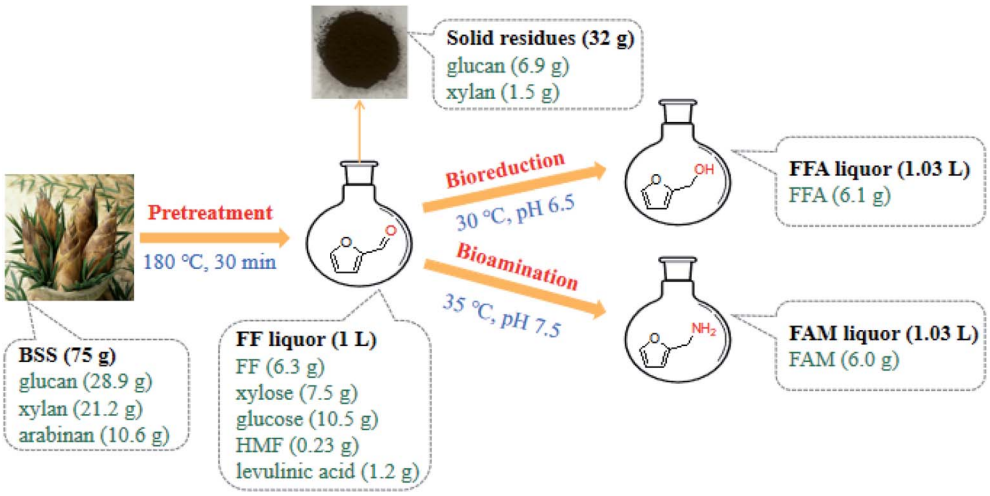

Fig. 8 Mass balance analysis for tandemly converting BSS into FFA or FAM (from BSS to furans).

90.3 mM FF was biologically aminated into FAM at 74% yield by the ω-transaminase biocatalyst using a high dose of amine donor D-alanine (1.44 M).[20] Excessive D-alanine was used for FF bioamination, and a large amount of unwanted byproduct pyruvate might produce, which was not easy to be isolated from the bioamination system. IPA was used as an amine donor; however, acetone was formed as a co-product after bioamination, which could be easily separated under a low pressure or slight heating. Clearly, a relatively low dose of the amine donor IPA was used, and high bioamination efficiency was achieved in this study.

To sum up, the whole cells of CCZU-A13 and AT2018 could be used to efficiently catalyze FF into furan chemicals under the mild performance conditions. Using the BSS-derived FF liquor as the feedstock, no inhibition was found when bioreduction with CCZU-A13 whole cells and bioamination with AT2018 whole cells. The combination of the heterogeneous Sn–graphite catalysis and biocatalysis in a cascade fashion without the isolation of intermediates and Sn–graphite catalysts could shorten the operating time, operation cost, and waste generation. Sustainable bioconversion of BSS-derived FF into high-value-added bio-furan chemicals was successfully verified in this study.

3.4. Mass balance from BSS to FFA and FAM

Mass balance was calculated using data from the BSS components, Sn–graphite-mediated catalysis of BSS to FF and whole-cell biocatalysis of FF (Fig. 8). The dry solid BSS (75.0 g) was composed of 28.9 g glucan, 10.6 g arabinan, and 21.2 g xylan. In a 5 L reactor containing 1 L deionized water, 75.0 g BSS, and 36.0 g Sn–graphite, the Sn–graphite-mediated catalysis of BSS was carried out for 30 min 500 rpm and 180 °C, and the obtained 1.0 L FF liquor was composed of 10.5 g glucose (58.3 mM), 7.5 g xylose (50.0 mM), 6.3 g FF (66.0 mM), 0.23 g HMF (1.8 mM) and 1.2 g levulinic acid (10.3 mM). BSS-derived FF (6.3 g) was bioconverted into 6.1 g FFA with the CCZU-A13 wet cells (50.0 g) within 2 h in the presence of 11.9 g glucose at 30 °C and pH 6.5. The yield was obtained at 0.142 g FFA per g BSS (0.310 g FFA per g xylan in BSS). Moreover, the 1.0 L BSS-derived FF liquor containing 6.3 g FF was biotransformed into 6.0 g FAM with the AT2018 wet cells (50.0 g) within 1.5 h by supplementary of 11.7 g IPA at 35 °C and pH 7.5. The yield was obtained at 0.140 g FAM per g BSS (0.305 g FAM per g xylan in BSS).

Lignocellulosic materials are regarded as sustainable feedstocks for manufacturing biobased chemicals.[46–50] Recently, these materials have gained a considerable interest to synthesize organonitrogen and hydroxy compounds from biomass feedstocks.[51–55] Organonitrogen chemical FAM and hydroxy compound FFA, two kinds of important furan molecules,[51–53] could be manufactured from the abundant, renewable and inexpensive BSS. First, BSS was effectively catalyzed to FF with Sn–graphite (3.6 wt% dosage) within 30 min at 180 °C. Subsequently, the bioreduction and bioamination of BSS-derived FF were conducted under mild reaction conditions. In a one-pot manner, the established chemoenzymatic approaches could be used for tandemly converting BSS into furan-based chemicals (furfuryl alcohol and furfurylamine) *via* a sequential catalysis with heterogeneous Sn–graphite catalysts and biocatalysts. This strategy might provide an economic way for high-value utilization lignocellulosic biomass, and a techno-economic analysis of the chemoenzymatic conversion of biomass into furan-based chemicals will be carried out in future research.

4. Conclusion

Using BSS as a feedstock, a high FF yield of 41.1% (based on the xylan in BSS) was obtained using the heterogeneous Sn–graphite catalyst (3.6 wt% dosage) in water (pH 1.0) at 180 °C for 30 min. BSS (75 g L^{-1}) could effectively convert xylan in BSS into 66.0 mM FF. Using glucose as a co-substrate, this BSS-derived FF could be catalyzed into FFA in the yield of 0.310 g FFA per g xylan in BSS by CCZU-A13 whole cells within 2 h at pH 6.5 and 30 °C. Using IPA as an amine donor, this BSS-derived FF

could be bioconverted into FAM in the yield of 0.305 g FAM per g xylan in BSS by AT2018 whole cells within 1.5 h at pH 7.5 and 35 °C. A sustainable and effective route for catalyzing biomass into FFA and FAM was successfully established *via* sequential chemical catalysis and biocatalysis.

Conflicts of interest

The authors declare no competing financial interest.

Acknowledgements

All authors gratefully acknowledge the financial support from the NSFC (National Natural Science Foundation of China) (21978072), the Open Project of State Key Laboratory of Biocatalysis and Enzyme Engineering (China), and the Open Project of Jiangsu Key Laboratory for Biomass-Based Energy and Enzyme Technology (BEETKB1902).

References

1 H. Li, X. Chen, J. i. Ren, H. Deng, F. Peng and R. Sun, *Biotechnol. Biofuels*, 2015, **8**, 127.
2 L. T. Mika, E. Cséfalvay and Á. Németh, *Chem. Rev.*, 2018, **118**, 505–613.
3 J. J. Bozell and G. R. Petersen, *Green Chem.*, 2010, **12**, 539–554.
4 C. M. Cai, T. Zhang, R. Kumar and C. E. Wyman, *J. Chem. Technol. Biotechnol.*, 2014, **89**, 2–10.
5 L. Y. Ye, J. M. Zhang, J. Zhao and S. Tu, *Bioresour. Technol.*, 2014, **153**, 147–153.
6 J. Q. Bond, A. A. Upadhye, H. Olcay, G. A. Tompsett, J. Jae, R. Xing, D. M. Alonso, D. Wang, T. Zhang, R. Kumar, A. Foster, S. M. Sen, C. T. Maravelias, R. Malina, S. R. H. Barrett, R. Lobo, C. E. Wyman, J. A. Dumesic and G. W. Huber, *Energy Environ. Sci.*, 2014, **7**, 1500–1523.
7 L. Zhang, H. Yu, P. Wang, H. Dong and X. Peng, *Bioresour. Technol.*, 2013, **130**, 110–116.
8 S. Peleteiro, S. Rivas, J. L. Alonso, V. Santos and J. C. Parajó, *Bioresour. Technol.*, 2016, **202**, 181–191.
9 A. S. Mamman, J. M. Lee, Y. C. Kim, I. T. Hwang, N. J. Park, Y. K. Hwang, J. S. Chang and J. S. Hwang, *Biofuels, Bioprod. Biorefin.*, 2008, **2**, 438–454.
10 A. O. Iroegbu and S. P. Hlangothi, *Chem. Afr.*, 2019, **2**, 223–239.
11 X. Y. Zhang, Z. H. Xu, M. H. Zong, C. F. Wang and N. Li, *Catalysts*, 2019, **9**, 70.
12 B. M. Nagaraja, V. Siva Kumar, V. Shasikala, A. H. Padmasri, B. Sreedhar, B. David Raju and K. S. Rama Rao, *Catal. Commun.*, 2003, **4**, 287–293.
13 Y. Yang, L. Chen, Y. Chen, W. Liu, H. Feng, B. Wang, X. Zhang and M. Wei, *Green Chem.*, 2019, **21**, 5352–5362.
14 M. Qiu, T. Guo, D. Li and X. Qi, *Appl. Catal., A*, 2020, **602**, 117719.
15 X. Liu, Y. Wang, S. Jin, X. Li and Z. Zhang, *Arabian J. Chem.*, 2020, **13**, 4916–4925.
16 M. Chatterjee, T. Ishizaka and H. Kawanami, *Green Chem.*, 2016, **18**, 487–496.
17 M. Pelckmans, T. Renders, S. Vande Vyver and B. F. Sels, *Green Chem.*, 2017, **19**, 5303–5331.
18 C. L. Dong, H. T. Wang, H. C. Du, J. B. Peng, Y. Cai, S. Guo, J. L. Zhang, C. Smart and M. Y. Ding, *Mol. Catal.*, 2020, **482**, 110755.
19 T. Gu, B. Wang, Z. Zhang, Z. Wang, G. Chong, C. Ma, Y. Tang and Y. He, *Process Biochem.*, 2019, **80**, 112–118.
20 X. L. Liao, Q. Li, D. Yang, C. L. Ma, Z. B. Jiang and Y. C. He, *Appl. Biochem. Biotechnol.*, 2020, **192**, 794–811.
21 C. Y. Bu, Y. X. Yan, L. H. Zou, Z. J. Zheng and J. Ouyang, *Bioresour. Technol.*, 2020, **313**, 123705.
22 M. Inagaki and T. Suwa, *Carbon*, 2001, **39**, 915–920.
23 T. Ndlovu, A. T. Kuvarega, O. A. Arotiba, S. Sampath, R. W. Krause and B. B. Mamba, *Appl. Surf. Sci.*, 2014, **300**, 159–164.
24 S. Mitra, K. S. Lokesh and S. Sampath, *J. Power Sources*, 2008, **185**, 1544–1549.
25 Y. J. Yang, E. H. Liu, L. M. Li, Z. Z. Huang, H. J. Shen and X. X. Xiang, *J. Alloys Compd.*, 2009, **487**, 564–567.
26 A. Morana, G. Squillaci, S. M. Paixao, L. Alves, F. La Cara and P. Moura, *Energies*, 2017, **10**, 1504.
27 L. Gong, Z. Y. Xu, J. J. Dong, H. Li, R. Z. Han, G. C. Xu and Y. Ni, *Bioresour. Technol.*, 2019, **293**, 122065.
28 O. Ershova, J. Kanervo, S. Hellsten and H. Sixta, *RSC Adv.*, 2015, **5**, 66727–66737.
29 F. Delbecq, Y. Wang, A. Muralidhara, K. El Ouardi, G. Marlair and C. Len, *Front. Chem.*, 2018, **6**, 146–174.
30 R. Mariscal, P. Maireles-Torres, M. Ojeda, I. Sadaba and M. Lopez, *Energy Environ. Sci.*, 2016, **9**, 1144–1189.
31 A. Mittal, S. K. Black, T. B. Vinzant, M. O'Brien, M. P. Tucker and D. K. Johnso, *ACS Sustainable Chem. Eng.*, 2017, **5**, 94–5701.
32 F. Delbecq, Y. T. Wang and C. Len, *J. Mol. Catal. A: Chem.*, 2016, **423**, 520–525.
33 I. Agirrezabal-Telleria, F. Hemmann, C. Jäger, P. L. Arias and E. Kemnitz, *J. Catal.*, 2013, **305**, 81–91.
34 R. O'Neill, M. N. Ahmad, L. Vanoye and F. Aiouache, *Ind. Eng. Chem. Res.*, 2009, **48**, 4300–4306.
35 J. Lessard, J. F. Morin, J. F. Wehrung, D. Magnin and E. Chornet, *Top. Catal.*, 2010, **53**, 1231–1234.
36 A. S. Dias, M. Pillinger and A. A. Valente, *J. Catal.*, 2005, **229**, 414–423.
37 X. Shi, Y. Wu, H. Yi, G. Rui, P. Li, M. Yang and G. Wang, *Energies*, 2011, **4**, 669.
38 I. Agirrezabal-Telleria, A. Larreategui, J. Requies, M. B. Güemez and P. L. Arias, *Bioresour. Technol.*, 2011, **102**, 7478–7485.
39 M. N. Catrinck, P. S. Barbosa, H. R. O. Filho, R. S. Monteiro, M. H. P. Barbosa, R. M. Ribas and R. F. Teófilo, *Fuel Process. Technol.*, 2020, **207**, 106482.
40 H. L. Li, J. L. Ren, L. J. Zhong, R. C. Sun and L. Liang, *Bioresour. Technol.*, 2015, **176**, 242–248.
41 R. Weingarten, G. A. Tompsett, W. C. Conner and G. W. Huber, *J. Catal.*, 2011, **279**, 174–182.

42 Y. M. Li, X. Y. Zhang, N. Li, P. Xu, W. Y. Lou and M. H. Zong, *ChemSusChem*, 2017, **10**, 372–378.
43 A. Dunbabin, F. Subrizi, J. M. Ward, T. D. Sheppard and H. C. Hailes, *Green Chem.*, 2017, **19**, 397–404.
44 F. F. Chen, Y. H. Zhang, Z. J. Zhang, L. Liu, J. P. Wu, J. H. Xu and G. W. Zheng, *J. Org. Chem.*, 2019, **84**, 14987–14993.
45 J. D. Zhang, J. W. Zhao, L. L. Gao, H. H. Chang, W. L. Wei and J. H. Xu, *J. Biotechnol.*, 2019, **290**, 24–32.
46 K. Yan, G. Wu, T. Lafleur and C. Jarvis, *Renewable Sustainable Energy Rev.*, 2014, **38**, 663–676.
47 D. Vargas-Hernández, J. M. Rubio-Caballero, J. Santamaría-González, R. Moreno-Tost, J. M. Mérida-Robles, M. A. Pérez-Cruz, A. Jiménez-López, R. Hernández-Huesca and P. Maireles-Torres, *J. Mol. Catal. A: Chem.*, 2014, **383–384**, 106–113.
48 J. Wang, X. Liu, B. Hu, G. Lu and Y. Wang, *RSC Adv.*, 2014, **4**, 31101–31107.
49 G. W. Huber, S. Iborra and A. Corma, *Chem. Rev.*, 2006, **106**, 4044–4098.
50 N. Araji, D. D. Madjinza, G. Chatel, A. Moores, F. Jerome and K. De Oliveira Vigier, *Green Chem.*, 2017, **19**, 98–101.
51 Y. Liu, K. Zhou, H. Shu, H. Liu, J. Lou, D. Guo, Z. Wei and X. Li, *Catal. Sci. Technol.*, 2017, **7**, 4129–4135.
52 C. L. Dong, H. T. Wang, H. C. Du, J. B. Peng, Y. Cai, S. Guo, J. L. Zhang, C. Smart and M. Y. Ding, *Mol. Catal.*, 2020, **482**, 110755.
53 S. Nishimura, K. Mizuhori and K. Ebitani, *Res. Chem. Intermed.*, 2016, **42**, 19–30.
54 S. Song, V. F. K. Yuen, L. Di, Q. Sun, K. Zhou and N. Yan, *Angew. Chem., Int. Ed.*, 2020, **59**, 19846–19850.
55 X. Chen, Y. Liu and J. Wang, *Ind. Eng. Chem. Res.*, 2020, **59**, 17008–17025.